Near-threshold study of the polarization of rare-gas resonance radiation: Neon

C. Norén* and J. W. McConkey
Department of Physics, University of Windsor, Windsor, Ontario, Canada N9B 3P4
(Received 28 November 1995)

The linear polarization of resonance vacuum-ultraviolet radiation emitted by electron-impact excited Ne atoms has been measured in the energy range from threshold to 21 eV. An electron resolution of 80 meV has enabled the effects of negative-ion resonances on the polarization function to be examined in some detail. Predictions of the effects of negative-ion resonances on the observed polarizations have been made using a generalized Baranger-Gerjuoy theory. Excitation via electron exchange is shown to be the dominant process very close to threshold.

PACS number(s): 34.80.Dp, 42.25.Ja

I. INTRODUCTION

The importance of the polarization of optical radiation is being increasingly recognized in a variety of fields [1,2]. These include absolute calibration of spectroscopic equipment, plasma diagnostics, astrophysics, and electron-impact excitation studies. Clearly, when considering electron-impact excitation of atoms or molecules, the polarization of the resultant radiation carries important information about the process itself. This is likely to be particularly important near threshold where conservation of angular momentum and its components in the quantization (electron-beam) direction allows accurate predictions about the magnitude of the polarization in this energy region. Previous reports of near-threshold polarization of electron-impact radiation have all been confined to the visible or near-uv spectral regions (see the review by Heddle and Gallagher [3], which gives references to earlier work).

Polarizations are difficult to measure in the near-threshold region not only because of low radiation intensities and the influence of cascade but also because of the perturbing effect of negative-ion resonances in this energy region [4]. Comparison with the theoretically predicted threshold values in the past has often been limited to extrapolated experimental data.

In an earlier publication [5] from this laboratory we presented data on the polarization of the vacuum ultraviolet (vuv) resonance radiation from He and Ne targets over an energy range from threshold to 500 eV obtained with an electron beam energy resolution of ~ 1 eV. Very recently, in the first paper [6] of this series (hereafter referred to as I), we presented higher-resolution near-threshold data for He. The present paper presents our higher-resolution near-threshold data for Ne.

II. BASIC THEORY

In paper I an outline has been given of the development of the basic theory of atomic line polarizations for LS-coupled systems based on the work of Percival and Seaton [7], Blum [8], and others. General expressions for the threshold polarization and the relevant perturbation coefficients were given.

For the heavy rare gases LS coupling is not valid and instead a coupling scheme referred to as jLS coupling has been successfully used. Here the orbital angular momentum L of the excited electron is coupled to the total angular momentum j of the ion core to form an intermediate state K, which in turn is coupled to the excited electron's spin S to form the total angular momentum J of the atom. The notation for describing these states is $(^{2s+1}l_j)\ ^{2S+1}L[K]_J$, where l and s are the orbital and spin angular momentum of the ion core, respectively. However, the lowest vuv emitting states $(J=1)$ can be considered as an admixture of ^1P and ^3P LS-coupled states and are represented as

$$|(^2P_{1/2})\ ^1S[\tfrac{1}{2}]_1\rangle = 0.964|^1P\rangle + 0.266|^3P\rangle,$$
$$|(^2P_{3/2})\ ^1S[\tfrac{3}{2}]_1\rangle = -0.226|^1P\rangle + 0.964|^3P\rangle. \quad (1)$$

It can be seen that the state with the $j=1/2$ core is predominantly ^1P in nature while the state with the $j=3/2$ core is predominantly ^3P.

Since LS coupling is not valid, only the total angular momentum is considered. For $J=0 \leftrightarrow J=1$ excitation decay (as is the case with the resonance lines of Ne, Ar, Kr, and Xe) the conservation of the z component of angular momentum requires that

$$M_J + m_l + m_s = M_J' + m_l' + m_s' \quad (2)$$

be satisfied where M_J (M_J') is the total angular-momentum magnetic quantum number before (after) electron impact, m_l (m_l') is the projection of the orbital angular momentum of the incident (scattered) electron onto the quantization axis, and m_s (m_s') is the projection of the spin of the incident (scattered) electron onto the quantization axis. If the incident electron defines the quantization axis, it has no angular momentum about this axis and thus $m_l=0$. Also, since the atom is initially in a $J=0$ state, $M_J=0$. At threshold the scattered electron carries off no energy and therefore no angular momentum (i.e., $m_l'=0$), which results in M_J' being determined by the electron spin. For direct excitation $m_s=m_s'$ and therefore $M_J'=0$ and thus $\Delta M_J=0$, which results in only parallel

*Present address: MS183-601, Jet Propulsion Laboratory, Pasadena, CA 91109.

polarized light ($I_{\parallel}$) being produced [6]. Since the polarization is defined as $(I_{\parallel}-I_{\perp})/(I_{\parallel}+I_{\perp})$ (see Sec. IV), this leads to a threshold polarization $P_{\rm th}$ of unity. For exchange excitation there are two possible outcomes: (i) $m_s=m_s'$ and (ii) $m_s=-m_s'$ (see [9]). For case (i) $M_J'=0$ (singlet excitation), the situation is indistinguishable from direct excitation and the resultant radiation is parallel polarized ($P_{\rm th}=+1$). For case (ii) $M_J'=\pm 1$ (triplet excitation) and therefore the resultant radiation is perpendicularly polarized, which gives a threshold polarization of -1. Note that $M_J'=\pm 1$ is excited only through exchange excitation. Thus a measurement of the polarization at threshold for the heavy rare gases will determine which mechanism is dominating. For mercury, which also has a $^1S_0$ ground state, exchange was observed to be dominant at energies close to threshold [10].

Note that the above considerations have not taken into account the hyperfine structure due to the presence of nuclear spin (**I**) from naturally occurring isotopes, which tends to depolarize the radiation. However, neon only has 0.257% of isotopes with nonzero **I** and therefore this will not be a significant factor.

If a temporary negative-ion resonance occurs close to threshold then we note that coupling will occur between the two electrons involved, thus causing angular momenta to be transferred between the different components on the right-hand side of Eq. (2). This causes the near-threshold arguments given above to be invalid and hence we expect resonance features to show up as perturbations in the polarization curves. Cascade [6] and electron correlation [11] effects can also have a significant effect on observed polarizations.

III. NEGATIVE-ION RESONANCES

Negative-ion formation has been thoroughly reviewed by Buckman and Clark [12] and the reader is referred to this article for a comprehensive review of the field. In this work the incoming electron interacts with the atomic target to form a relatively long-lived negative-ion state (i.e., significantly longer than the transit time of the electron across the atom), which then decays via electron emission to a free electron and an excited atom. This process competes with the direct process and this interference leads to distinct spectral features at the location of the resonance.

The scheme used to describe the negative-ion resonances for the heavy rare gases is referred to as the ''grandparent'' model and was developed by Read, Brunt, and King [13]. In this scheme the resonances are associated with the ground or an excited state of the neutral target atom (referred to as the ''parent'' state). If the parent state is an excited state (*core-excited* resonance) then the ion core is referred to as the grandparent state. For example, in the heavy rare gases some resonances are of the type $\ldots np^5\,{}^2P_{3/2}n'ln''l$, where $\ldots np^5\,{}^2P_{3/2}n'l$ is the parent state and $\ldots np^5\,{}^2P_{3/2}$ is the grandparent state. Their proposal treats the two outermost electrons $(\boldsymbol{l}_1,\mathbf{s}_1;\boldsymbol{l}_2,\mathbf{s}_2)$ as a correlated pair and therefore more strongly coupled to each other than either one is to the ion core. Since the interaction between the excited electrons is mostly electrostatic, the orbital and spin angular momentum couple separately (i.e., LS coupling): $\boldsymbol{l}_1+\boldsymbol{l}_2=\mathbf{L}$ and $\mathbf{s}_1+\mathbf{s}_2=\mathbf{S}$. By analogy with the jLS coupling scheme for the neutral excited states of the rare gases, the ion core angular momentum **j** is coupled with **L** to form the intermediate state $\mathbf{K}(\mathbf{j}+\mathbf{L}=\mathbf{K})$, which in turn is coupled with **S** to form the total angular momentum $\mathbf{J}(\mathbf{K}+\mathbf{S}=\mathbf{J})$. The resonance is classified using a nomenclature that is also similar to that of the neutral excited states: $(j)\,{}^{2S+1}L[K]_J$. Calculations by Noro, Sasaki, and Tatewaki [14], Ohja, Burke, and Taylor [15], and Clark and Taylor [16] have shown that the jLS coupling is appropriate for neon and argon.

The different classes of resonances observed were assigned to a particular configuration and each configuration was designated with a latin letter [13]. For example, the letter b corresponds to the following configuration: $b_{1,2}\equiv np^5\,{}^2P^o_{3/2,1/2}(n+1)s(n+1)p\,{}^3P^o$. Note that the final term only refers to the coupling of the outer electrons. It can be seen from $b_{1,2}$ that the negative-ion resonances consist of a multiplet of states (except when the outer electrons couple to form a ^1S state). In the discussion that follows only resonances relevant to the present study are discussed. The reader is referred to [13] and [12] for a more complete discussion of all resonances.

The b resonances lie just above the inelastic threshold of their parent states, which would classify them as shape resonances. However, there is evidence that the resonances could also be classified as Feshbach [12]. In either case, the resonance feature is expected to be sharp.

The coupling of the $(n+1)s(n+1)p\,{}^3P$ electrons with j of the ion core produces considerable fine structure. The total number of states that can be produced is 13 (8 when $j=3/2$ and 5 when $j=1/2$); however, several of these states will likely be undetectable. Since these states are of even parity they can be formed by the ground-state atom interacting with $s_{1/2}$ or $d_{3/2,5/2}$ electrons (assuming no electrons with partial waves $l\geqslant 4$). This restricts the total angular momentum of the resonance to be $\leqslant 5/2$ since the initial angular momentum of the target atom is 0 and therefore eliminates one of the eight states associated with $j=3/2$ ion core. Also four of the resonances are associated with the process

$$e^-(ks)+\mathrm{Ne}(np)\rightarrow \mathrm{Ne}^-[(n+1)s(n+1)p]\rightarrow e^-(ks)+\mathrm{Ne}^*[(n+1)p], \tag{3}$$

which involves only a change in the principle quantum number. These resonances are expected to be short lived and therefore produce broad features that are difficult to detect experimentally. This leaves eight resonances that can be formed by d-wave excitation, three based on the $^2P_{1/2}$ core and five on the $^2P_{3/2}$ core [13]. All these states can decay through p-wave emission.

The $3s3p$ electrons can also couple to form a ^1P term (i.e., the c resonances), which is split into five states by analogy with alkaline-earth elements. These resonances are expected to lie higher in energy than the ^3P (b) resonances. All these states can decay through p-wave emission to the $np^5(n+1)s$ manifold without rearrangement of the $(n+1)s$ electron and therefore the resonances are broad.

To determine the effect of the resonances on the polarization function the scattering amplitude needs to be calculated for the above processes. This can be done using the method outlined by Wolcke *et al.* [17], which is a generalization of

the Baranger-Gerjuoy theory [18], for mercury where the scattering amplitude is expressed in terms of only 3-j symbols.

As in mercury, the ground state for all rare gases is $^1S_0$ and is represented by the state vector $|0\rangle$. The quantization axis lies parallel to the electron momentum vector. The excited state is described by the grandparent scheme (i.e., jLS coupling) discussed above and the incident (scattered) electron is described by momentum $\mathbf{p}_0$ ($\mathbf{p}_1$), spin $\mathbf{s}_0$ ($\mathbf{s}_1$), and spin z component m_{s_0} (m_{s_1}). The scattering amplitude is given by

$$f(M_J,m_{s_1},m_{s_0})=\langle[(j,L)K,S]JM_J;\mathbf{p}_1 s_1 m_{s_1}|\mathbf{T}|0;\mathbf{p}_0 s_0 m_{s_0}\rangle. \tag{4}$$

The electron momentum vectors $(\mathbf{p}_0,\mathbf{p}_1)$ are now expanded in terms of partial waves with orbital angular momentum (l_0,l_1). Unlike the mercury atom where $\boldsymbol{l}$ and $\mathbf{s}$ for each electron were coupled, the heavy rare gases couple $\boldsymbol{l}_1$ and $\mathbf{L}$ to form $\mathbf{L}'$, and $\mathbf{s}_1$ and $\mathbf{S}$ to form $\mathbf{S}'$. To do this we must first uncouple $\mathbf{L}$ and $\mathbf{S}$ from $\mathbf{J}$ and then $\boldsymbol{l}_1,\mathbf{L}$ and $\mathbf{s}_1,\mathbf{S}$ can be coupled to form $\mathbf{L}'$ and $\mathbf{S}'$, respectively. Finally, $\mathbf{L}'$ is coupled to $\mathbf{j}$ to form $\mathbf{K}'$, which is then coupled to $\mathbf{S}'$ to obtain the total angular momentum ($\mathbf{J}'$) of the negative-ion resonance. The initial state of the electron-atom system before the collision can be described by coupling $\boldsymbol{l}_0$ and $\mathbf{s}_0$ to form $\mathbf{j}_0$ ($=\mathbf{J}'$). The scattering amplitude for the negative-ion state $(j)\,{}^{2S'+1}L'[K']_{J'}$ then becomes

$$\begin{aligned}f(M_J,m_{s_1},m_{s_0})&=\langle[(j,L)K,S]JM_J;l_1 m_{l_1},s_1 m_{s_1}|\mathbf{T}|0;l_0 m_{l_0},s_0 m_{s_0}\rangle\\&=\sum_x (l_0 m_{l_0},s_0 m_{s_0}|j_0 m_{j_0})(KM_K,SM_S|JM_J)(jM_j,LM_L|KM_K)(LM_L,l_1 m_{l_1}|L'M_{L'})(SM_S,s_1 m_{s_1}|S'M_{S'})\\&\quad\times(jm_j,L'M_{L'}|K'M_{K'})(K'M_{K'},S'M_{S'}|J'M_{J'})\langle[(j,L')K',S']J'M_{J'}|\mathbf{T}|(l_0 s_0)j_0 m_{j_0}\rangle\mathbf{C}(\mathbf{p}_1 l_1 m_{l_1},\mathbf{p}_0 l_0),\end{aligned} \tag{5}$$

where x represents $l_0,l_1,j_0,m_{j_0},M_K,M_S,M_L,m_j,L',M_{L'},S',M_{S'},K',M_{K'},J',M_{J'}$ and the terms from the partial-wave expansion are contained in $\mathbf{C}(\mathbf{p}_1 l_1 m_{l_1},\mathbf{p}_0 l_0)$. Note that (i) $J'=j_0$ because the total angular momentum is conserved, (ii) $M_{J'}=m_{j_0}$ because the $\mathbf{T}$-matrix element is independent of $M_{J'}$, and (iii) $m_{j_0}=m_{s_0}$ because $\mathbf{p}_0$ defines the quantization axis and therefore $m_{l_0}=0$.

Since the negative-ion states are specified by $(j)\,{}^{2S'+1}L'[K']_{J'}$ this reduces the number of terms to be summed in (5). Also, conservation of angular momentum and parity restrict l_0 to only one possible value and since the excitation is close to threshold only the lowest values of l_1 will be considered. The properties of the Clebsch-Gordan coefficients restrict the values that the angular-momentum z components can have since (i) m_{s_0}, m_{s_1}, and M_J are fixed for each scattering amplitude (denoted α, β, and γ, respectively), (ii) $M_{J'}=m_{j_0}$, and (iii) $m_{l_0}=0$,

$$\begin{gathered}m_{l_1}=\alpha-\beta-\gamma,\quad M_K=\gamma-M_S,\quad m_j=\gamma-M_S-M_L,\\M_{L'}=M_L+\alpha-\beta-\gamma,\quad M_{S'}=M_S+\beta,\\M_{K'}=\alpha-\beta-M_S.\end{gathered} \tag{6}$$

The net result is that the summation in Eq. (5) has been reduced to two terms (M_L and M_S). Note that the above calculation does not allow for a change in the core angular momentum j. If j is uncoupled and then recoupled to form the new core state j', this leads to the scattering amplitude being zero for $j\neq j'$ because of the following property for Clebsch-Gordan coefficients [19]:

$$\sum_{m_s,m_l}(sm_s,lm_l|jm_j)(sm_s,lm_l|j'm_{j'})=\delta_{jj'}\delta_{m_j,m_{j'}}. \tag{7}$$

If a change in core angular momentum occurs, configuration interaction may be used to more accurately describe the negative resonance and neutral excited state [20].

The vuv polarization fraction may be calculated using (5) above with Eqs. 4, 5b, 13a, and 13b from Bartschat *et al.* [21]. Note that Eqs. 4 and 5b from Ref. [21] must be integrated over all scattering angles. As in the case of mercury, the $\mathbf{T}$ matrix and $\mathbf{C}(\mathbf{p}_1 l_1 m_{l_1},\mathbf{p}_0 l_0)$ can be neglected since they are common to all scattering amplitudes being considered and thus will divide out in the polarization calculation. The results for various negative ion resonances (where no change in the ion core angular momentum occurs) are shown in Tables I ($j=1/2$) and II ($j=3/2$).

The preceding derivation of the polarization fractions due to negative-ion resonances was based on the assumption that resonance formation was the dominating channel. This assumption would only be valid near threshold where the nonresonant excitation cross section is small. However, when the nonresonant excitation channel becomes comparable to the resonance channel both scattering amplitudes must be considered, which leads to interference effects between the two channels. Thus, away from the threshold region the predicted polarization values (Tables I and II) should be considered only as a first correction to the polarization function. If the resonance produces positively polarized radiation the $I_\parallel$ channel is expected to be enhanced relative to the $I_\perp$ channel and vice versa for resonances that produce negatively polar-

TABLE I. vuv polarization fractions for the heavy rare gases resulting from the formation of the negative-ion resonance $(j=1/2)\ ^{2S+1}L[K]_J$, which decays to $(j=1/2)\ ^2S[\frac{1}{2}]_1$.

Resonant state $(j=1/2)$	K	J	l_0	l_1	Polarization $(\overline{G_2}=1)$
^3P (b and e)	1/2	1/2	0	1	0
	3/2	1/2	0	1	0
	1/2	3/2	2	1	−0.428
	3/2	3/2	2	1	0.558
	3/2	5/2	2	1	0.500
^1P (c)	1/2	1/2	0	1	0
	3/2	3/2	2	1	0
^1S (d and f)	1/2	1/2	1	0	0
^1D (e)	3/2	3/2	1	2	0
	5/2	5/2	3	2	0

ized radiation. The shape of the resonance cannot be determined since the polarization fraction only gives a measure of the relative difference between the $I_\parallel$ and $I_\perp$ channels.

It should also be noted that above threshold there are often several resonances and neutral states that lie in the same energy region and thus the polarization analysis becomes very complicated. Earlier measurements of total electron-impact excitation functions can be used to determine which channels are the dominant ones and thus simplify the analysis.

IV. EXPERIMENT

A full discussion of the apparatus is presented in I and therefore only details relevant to the present measurement are discussed here. Electrons were energy selected using a hemispherical analyzer and focused through a target gas beam into a Faraday cup. Currents were typically 4 nA with an energy spread of approximately 80 meV.

The polarization P of the radiation is defined in the usual way as $(I_\parallel - I_\perp)/(I_\parallel + I_\perp)$, where $I_\parallel$ and $I_\perp$ are the true intensities measured in a direction orthogonal to the electron beam. The measured intensities $(I'''_\parallel, I'''_\perp)$ are related to the true values $(I_\parallel, I_\perp)$ by Eq. (6) from I. The efficiency η of the polarizer was obtained by normalizing our polarization data using the earlier measurements of Hammond *et al.* [5] and Karras [22], where they used multiple mirror polarizers to make the measurements insensitive to the mirror efficiency. The normalization was carried out at an energy of 40 eV, where the data were unperturbed by resonance effects and where the polarization was a relatively slowly varying function with impact energy. A value of 0.526 was obtained for η.

Studies of the variation of P with gas pressure were carried out to ensure freedom from depolarizing effects such as imprisonment of resonance radiation. This meant that the background pressure in the system did not exceed 6×10^{-7} Torr when the gas beam was operational. Background effects due, for example, to small contributions to the measured signals from the background gas in the system were accounted for as discussed by Hammond *et al.* [5]. The base pressure without the target gas being introduced was 2×10^{-7} Torr. Errors were estimated as discussed in I.

V. RESULTS

$I_\parallel$ and $I_\perp$ data, corrected as discussed earlier, are displayed in Fig. 1 and the resultant polarization curve is shown in Fig. 2. The sublevel cross section data were normalized using the data of Phelps *et al.* [26]. The observed polarization function agrees well in the region of overlap with previous measurements by Hammond *et al.* [5] and Uhrig *et al.* [23]. The only discrepancy is at threshold where Hammond *et al.* observe a value of 0.065, Uhrig *et al.* observe the polarization rise towards +1 as the electron-impact energy decreases (suggesting that direct excitation is predominant), and the present results show the polarization drop toward −1 as the impact energy decreases very close to threshold. The value obtained by Hammond *et al.* is consistent with the present results since their energy resolution (500 meV) would not permit the observation of the rapid decrease in polarization (a drop from 0 to −1 in 80 meV). The sharp increase in polarization observed by Uhrig *et al.* starts 300 meV above threshold and therefore Hammond *et al.* should

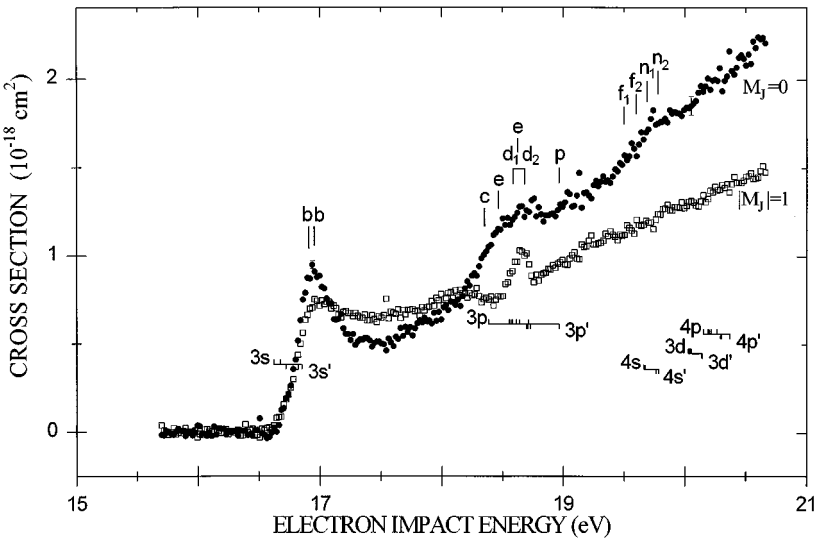

FIG. 1. Sublevel excitation functions for neon as a function of electron impact energy. Data were normalized using the results of Phelps *et al.* [26]. The data have been corrected for the polarization sensitivity of the analyzer. $M_J=0$ and $|M_J|=1$ curves refer to $I_\parallel$ and $I_\perp$, respectively (see the text). Positions of relevant negative-ion states are identified by lowercase letters [24,25] and are indicated above the curves. Positions of relevant neutral states are indicated below the curves.

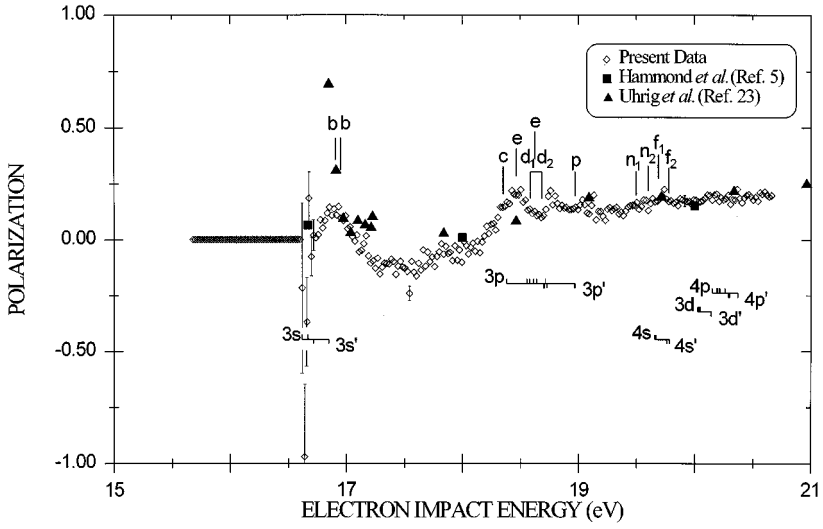

FIG. 2. Polarization function for the vuv radiation as a function of electron impact energy. Data from the lower resolution work of Hammond *et al.* [5] and Uhrig *et al.* [23] are indicated on the graph. Positions of relevant negative-ion states are identified by lowercase letters [24,25] and are indicated above the curves. Positions of relevant neutral states are indicated below the curves. Typical error limits are shown at threshold 17.5 and 20 eV and are discussed in the text.

have observed a larger polarization value than they measured at threshold if this effect was real. The data points below the threshold have been set to zero for the sake of clarity.

A. Effect of resonances from threshold to 18 eV

Both Figs. 1 and 2 clearly show that resonances and cascading from higher-lying states are perturbing the excitation of neon. Near threshold, where cascade from higher excited states is not a factor, it can be seen that the *b* resonances, observed in both the vuv [24] and metastable [25] spectra, are having a perturbing effect. This is in contrast to helium where the polarization was smoothly varying and no resonances were observed in the near-threshold region (see paper I).

The determination of the threshold polarization is complicated by the presence of the *b* resonances. The *b* resonance located at 16.95 eV has an estimated full width at half maximum of 180 meV [24] and with an electron beam resolution of 80 meV, it is clear that the effects of the *b* resonance can extend near the threshold of $np^5 3s[3/2]_1$ state. As noted above, the polarization is heading toward large negative values on the lower-energy side of the *b* resonance. This indicates that the exchange process is dominating at threshold [see Eq. (1) and the discussion thereafter], which is not unexpected since the lower state $np^5 3s[3/2]_1$ is predominantly ^3P in character and therefore requires exchange (i.e., spin flip) for excitation.

Above threshold, within the first 0.5 eV, it can be seen in Fig. 1 that the $I_\parallel$ channel is being enhanced relative to the $I_\perp$ channel. This is reflected in the polarization curve (Fig. 2) as a rapid increase to a peak value of ~ 0.13. The assertion that the dominating presence of the *b* resonance is causing this rapid change in polarization is supported by the polarization calculations presented earlier (see Tables I and II) where five of the possible *b* states have predicted polarizations close to 0.5. The fact that the observed peak polarization is ~ 0.13 rather than ~ 0.5 as predicted can be explained by (i) the energy resolution of the beam and/or (ii) the presence of several resonance states. If the energy resolution was poor enough to significantly convolute the resonance signal with the signal due to nonresonant excitation, then a decrease in polarization would be observed since the polarization arising from nonresonant excitation is negative in this region. Preliminary measurements with a poorer energy resolution have resulted in significantly reduced peak polarizations. Better electron energy resolution would presumably increase the observed peak polarization. Note that an accurate calculation of the combined polarization due to several resonances would require determining the interference effects between the different scattering amplitudes (cf. Sec. III). The fact that significant overall positive polarizations were observed suggests that the dominating resonances have *J* values of 3/2 and 5/2 (see Tables I and II).

The $np^5 3s[1/2]_1$ neutral state, which lies 177 meV above threshold, is predominantly ^1P in nature and thus excited by direct excitation with a threshold polarization value of $+1$ (cf. helium). Since the present experiment cannot discriminate against vuv radiation emitted from this state, any con-

TABLE II. vuv polarization fractions for the heavy rare gases resulting from the formation of the negative-ion resonance $(j=3/2)\ ^{2S+1}L[K]_J$, which decays to $(j=3/2)\ ^2S[\frac{3}{2}]_1$.

Resonant state ($j=3/2$)	K	J	l_0	l_1	Polarization ($\overline{G_2}=1$)
^3P (b and e)	1/2	1/2	1	1	0
	3/2	1/2	1	1	0
	1/2	3/2	1	1	−0.428
	3/2	3/2	1	1	−0.698
	5/2	3/2	1	1	0.447
	3/2	5/2	3	1	0.500
	5/2	5/2	3	1	0.500
^1P (c)	1/2	1/2	0	1	0
	3/2	3/2	2	1	0.143
	5/2	5/2	2	1	0.500
^1S (d and f)	3/2	3/2	1	0	0.600
^1D (e)	1/2	1/2	1	2	0
	3/2	3/2	1	2	−0.529
	5/2	5/2	3	2	−0.088
	7/2	7/2	3	2	0.455

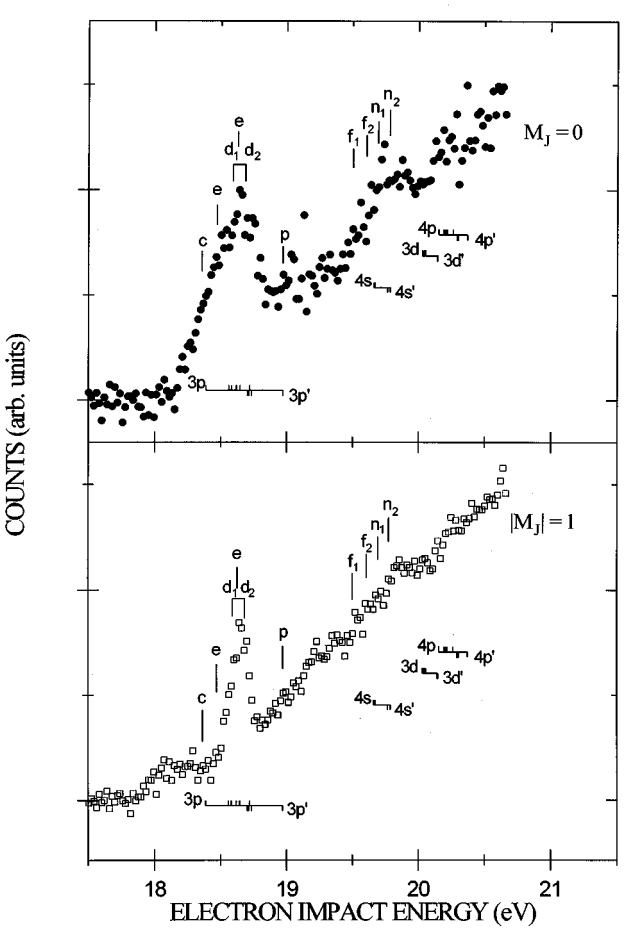

FIG. 3. Integrated vuv excitation functions for neon as a function of electron-impact energy with a linear function subtracted (see the text). Positions of relevant negative-ion states are identified by lowercase letters [24,25] and are indicated above the curves. Positions of relevant neutral states are indicated below the curves.

tribution to the polarization from its decay would be expected to bias its value toward $+1$. Since the observed polarization drops back to negative values (-0.15 at 17.25 eV) as the impact energy increases past the region where the *b* resonances influence the data, this is an indication that the ^3P component of the admixture is still dominating the excitation mechanism at energies between 17 and 18 eV. Above the *b* resonance, the polarization remains relatively flat up to 17.5 eV. At this point the polarization starts to rise again.

B. Effect of resonances on sublevel cross sections above 18 eV

To emphasize the less pronounced features in the $I_\perp$ and $I_\parallel$ channels more clearly, a straight line was determined from the data over the energy range of 17.5–17.86 eV for each spectrum (see Fig. 1) and was subtracted from the respective data sets. The results are presented in Fig. 3.

Measurements by Phelps *et al.* [26] on the excitation cross sections for the $np^5 3s[1/2]_1$ and the $np^5 3s[3/2]_1$ states at 18.2 eV show that the $np^5 3s[1/2]_1$ level is responsible for 81% of the total signal and therefore one could expect that resonances based on this state ($j=1/2$) should dominate (Table I). From Table I it can be seen that the polarization of the *c*, *d*, and *e* resonances is predominantly 0, indicating that the resonance structure should enhance both the $I_\perp$ and $I_\parallel$ channels equally. In the $I_\perp$ channel a broad dip is evident in the neighborhood of the *c* resonance (18.3 eV), which is not observed in the $I_\parallel$ channel, suggesting that this decays predominantly into the $I_\parallel$ channel. This behavior is not expected from resonances with a $j=1/2$ ion core but could be expected from the calculations for resonances based on a $j=3/2$ core (Table II). Thus it appears that either resonances based on the $j=3/2$ ion core are significant even though excitation to the corresponding neutral state is diminished or else the interference effects that have been considered negligible as a first approximation are in fact significant. Clearly it would be beneficial to have more detailed calculations performed. Note that the dip around 18.3 eV was also observed in the metastable channel and was designated a Wigner downstep by Buckman *et al.* [25].

Following the broad minimum, a strong peak is observed in the $I_\perp$ channel, most likely due to the effects of the *e* and/or *d* resonances in this region. We note from Tables I and II that certain *e* resonances should greatly enhance the $I_\perp$ channel leading to a dip in the observed polarization as is in fact observed. Because of the significance of the effect and the dominance of the $j=1/2$ ion core noted above, one might infer that the predominant resonance is the $^2P^o_{1/2}\,{}^3P[1/2]_{3/2}$ configuration with a predicted polarization of -0.428. Here the incoming and outgoing partial waves are a *d* wave and *p* wave, respectively. However, there are resonances with a $j=3/2$ ion core that also could cause the above effect (Table II).

In the $I_\parallel$ channel a broad feature is observed with an onset occurring at 18.16 eV. This is probably due to the combined effect of the *c* and *d* resonances both of which should preferentially enhance the $I_\parallel$ channel (Table II) if the $j=3/2$ core resonances are strong. This observation is supported by argon data [27], which again shows the *c* resonance having a strong effect.

Finally, between 19.45 and 20 eV another broad feature is observed in the $I_\parallel$ channel. In this region there are four resonances (n_1 n_2, f_1, and f_2) that were observed in the metastable spectrum [25] and four excited states [$4s(J=2,1)$ and $4s'(J=0,1)$]. We note that both *f* and *n* (also a ^1S state) resonances based on the $j=3/2$ core are expected to enhance the polarization and hence the $I_\parallel$ channel (see Table II).

C. Effect of resonances on the polarization function above 18 eV

The effects of the above resonances on the polarization can plainly be seen in Fig. 2. After the *b* resonance, the polarization curve falls to a minimum of -0.15 and then begins to rise toward zero over the energy range 17.5–18.15. The onset of the broad resonance at 18.16 eV in the $I_\parallel$ channel causes the polarization function to rise to a maximum of 0.2. The strong enhancement of the $I_\perp$ channel appears as a dip superimposed on this broad resonance (this effect is also seen in argon [27]) and therefore it seems unlikely that the *d* resonances are enhancing the $I_\parallel$ channel. The polarization resulting from the *d* resonances decaying directly to the $2p^5 3s$ state are given in Tables I and II, but Sharpton *et al.* [28] observed a sharp peak at 18.6 eV in the excitation function of the lowest-lying $2p^5 3p$ ($J=1$) state, which was attributed to these negative-ion resonances and

therefore it appears that this is a competing channel for decay of the d resonances. After the d_2 resonance, the polarization curve returns to its background value of 0.2 followed by a drop to a value of 0.1 as the electron energy is further increased. This could well be due to the depolarizing effect of the cascade feeding the $3s$ levels from the $3p$ states, which are known to be strongly excited in this region. As mentioned earlier in the discussion of $I_{\|}$, there are indications of resonance perturbations of the polarization near 19.5 eV probably due mainly to f resonances. The polarization then slowly rises to a value of 0.2 at 20.66 eV.

D. Influence of exchange excitation

As observed above, the exchange excitation mechanism is dominant at threshold but at higher energies direct excitation is expected to dominate. It is of interest to determine how the exchange excitation varies with respect to the direct excitation as a function of energy. To do this we start with the following definitions for the cross section:

$$\sigma^e = \tfrac{2}{3}(I^e_{\|} + 2I^e_{\perp}) = \tfrac{1}{3}(3 - P^e)(I^e_{\|} + I^e_{\perp}),$$
$$\sigma^d = \tfrac{1}{3}(3 - P^d)(I^d_{\|} + I^d_{\perp}), \tag{8}$$

where the superscripts e and d refer to exchange and direct, respectively. The measured polarization (P^m) can be written as

$$P^m = \frac{(I^d_{\|} + I^e_{\|}) - (I^d_{\perp} + I^e_{\perp})}{(I^d_{\|} + I^e_{\|}) + (I^d_{\perp} + I^e_{\perp})} = \frac{P^d(I^d_{\|} + I^d_{\perp}) + P^e(I^e_{\|} + I^e_{\perp})}{(I^d_{\|} + I^e_{\|}) + (I^d_{\perp} + I^e_{\perp})}. \tag{9}$$

Using Eq. (8), this results in

$$P^m = \frac{P^d(3\sigma^d)(3 - P^d)^{-1} + P^e(3\sigma^e)(3 - P^e)^{-1}}{(3\sigma^d)(3 - P^d)^{-1} + (3\sigma^e)(3 - P^e)^{-1}}. \tag{10}$$

Rearranging terms yields

$$\frac{\sigma^e}{\sigma^d} = \left(\frac{3 - P^e}{3 - P^d}\right)\left(\frac{P^d - P^m}{P^m - P^e}\right) \tag{11}$$

and using the relation $\sigma = \sigma^e + \sigma^d$ results in

$$\frac{\sigma^d}{\sigma} = \frac{1}{\left(\dfrac{(3 - P^e)}{(3 - P^d)}\dfrac{(P^d - P^m)}{(P^m - P^e)}\right) + 1}. \tag{12}$$

To proceed further the following assumptions are made.

(i) $P^e = -P^d$. This seems reasonable because, neglecting resonances and other perturbing effects, P^d is known (e.g., helium) to fall from $+1$ at threshold to smaller positive values as the energy is increased, whereas P^e is known to be -1 at threshold (e.g., mercury) and presumably also falling toward zero as E increases.

(ii) The polarization of the ''directly'' excited components was assumed to follow that of He($^1P_1$) excitation measured in I. Note that because in He the first eV above threshold is resonance and cascade free, it therefore provides a true ''direct'' polarization function. To determine the shape of the direct polarization function after the first eV, we must consider how it would look in the absence of cascade, which always leads to a depolarizing effect and thus the data of Steph and Golden [29], whose coincidence measurements are cascade free, are taken and a cubic spline technique was used to fit the near threshold data (from I) to theirs at 30 eV. The energy scale of the helium data was shifted so that the onset coincided with that of neon and the resultant curve is shown in Fig. 4(a).

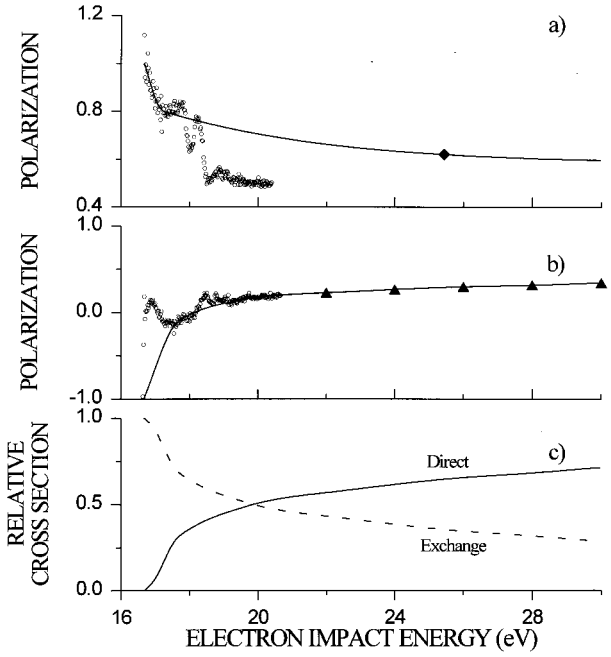

FIG. 4. (a) Polarization curve (solid line) resulting from direct excitation as determined from helium data in the manner outlined in the text. Circles, data of Norén *et al.* [6]; diamond, data of Steph and Golden [29]. Data points were shifted by 4.55 eV to coincide with the Ne threshold. (b) Estimated Ne polarization curve (solid line) in the absence of the negative-ion resonances. Circles, present data; triangles, data of Hammond *et al.* [5]. (c) Direct and exchange excitation functions relative to the total excitation function [see Eq. (12) and discussion following].

(iii) The measured polarization (P^m) is determined from the parts of the neon polarization data that are considered free from resonances and assuming a threshold value of -1. Note that no attempt has been made to correct for cascade, but considerable weight is put on the region between 17 and 18 eV, which is free of resonances and lies below the threshold for cascade.

In order to apply Eqs. (11) and (12) to obtain the relative contributions of the direct and exchange excitation, the measured polarization (P^m) must be determined. This was done by picking data points in resonance-free regions and performing a polynomial fit. Figure 4(b) shows the measured data with the polynomial line running from threshold ($P = -1$) through the 17–18 eV region and then to higher energies. Note that the resonance effects just above threshold have been neglected.

With the assumptions noted above the ratios σ^d/σ and σ^e/σ have been calculated and are plotted in Fig. 4(c). As noted above, the effect of cascade on the measured polarization has not been accounted for and would start becoming significant around 18 eV where a ''knee'' shape is observed in the relative cross sections [Fig. 4(c)]. It can be seen that the exchange mechanism (^3P excitation) dominates only in the first 1 eV and then the direct mechanism (^1P excitation) quickly becomes the predominant mode of excitation. As far as the excitation of the vuv emitting states is concerned, the excitation of the $np^5 3s[1/2]_1$ should quickly rise from zero to dominate the excitation process since it is predominantly ^1P in character (see Sec. III), while the excitation of the $np^5 3s[3/2]_1$ state should rapidly decrease above threshold. This behavior is supported by the wavelength resolved excitation measurements of Phelps *et al.* [26] and Phillips, Anderson, and Lin [30]. Their measurements involved exciting the neon atom by electron impact and then probing the excited states using a laser. Phelps *et al.* [26] used 18.2-eV electrons to excite neon so that they would not have to correct for cascade and from their data the ratio of the apparent excitation cross section of the $np^5 3s[1/2]_1$ (i.e., ^1P) state to the total apparent excitation cross section ($np^5 3s[1/2]_1 + np^5 3s[3/2]_1$) is 0.81. Phillips *et al.* [30] performed measurements at 40 eV and above, which required corrections for cascade from the higher-lying states. Using the measurements of Sharpton *et al.* [28] to correct for cascade they obtained a ratio of ~ 0.92 for the energy range 40–300 eV. Our prediction, from Fig. 4(c), is that at 18 eV about 30% of the excitation of the $J=1$ states is direct and about 70% is via exchange.

Given the uncertainties in our procedure, the agreement with Phelps *et al.* and Phillips, Anderson, and Lin is acceptable. It is not possible to make more detailed comparisons because of a number of factors. In our case we have measured the integrated emission from the two $J=1$ states, whereas they considered the two states separately. The Phelps *et al.* data were taken at 18.2 ± 0.5 eV, where cross sections are changing rapidly and thus the accuracy of the energy calibration becomes an important factor. Their work also involved the use of relatively high target pressures, where radiation trapping was complete and where, presumably, considerable collisional transfer effects must be occurring. We worked at very low pressures to ensure that no radiation trapping occurred.

Hanne *et al.* [10] have measured the polarization of the $6\ ^3P_1 - 6\ ^1S_0$ resonance line in coincidence with forward scattered electrons for mercury. The $6\ ^3P_1$ state is not a pure state, but contains a $6\ ^1P_1$ admixture (17.1%), which is similar to neon (7%) and argon (20%). Because the forward scattered electron is measured, the selection rule $\Delta M_J = 0$ is in effect. Using Eq. (2), one can immediately see that for $M_J = \pm 1$ to be excited, exchange ($\Delta M_S = \pm 1$) must occur and therefore a measurement of the polarization will determine whether exchange or direct excitation is occurring. Their results show that at threshold exchange excitation is dominating (i.e., the polarization is approaching the theoretical limit for pure exchange at threshold) and quickly rises over 2–3 eV above threshold toward the polarization limit for direct excitation. This result is in agreement with the present measurement that exchange excitation is dominant in the near-threshold region. Theoretical calculations by McConnell and Moiseiwitsch [31] (electrons scattered in all directions) and Bonham [32] (electrons scattered in forward direction) also show this trend.

VI. CONCLUSION

The polarization function for the integrated vuv radiation resulting from electron impact on Ne atoms has been measured in the threshold region. At threshold, the polarization function was observed to go toward large negative values, indicating that exchange excitation is dominant at threshold energies. Above threshold the perturbing effects of the negative-ion resonances on the polarization function can be seen, particularly from the *b* resonances. Predictions of the effects of the resonances on the observed polarization have been made using a generalized Baranger-Gerjuoy theory.

ACKNOWLEDGMENTS

The authors would like to thank K. Bartschat and P. Hammond for their helpful discussions. The authors are pleased to acknowledge financial assistance from the Natural Sciences and Engineering Research Council of Canada and expert technical help from the staff of the mechanical and electronic shops at Windsor.

[1] T. Fujimoto, F. Koike, K. Sakimoto, R. Okasaki, K. Kawasaki, K. Takiyama, T. Oda, and T. Kato, National Institute for Fusion Science Report No. NIFS-DATA-16, Nagoya, Japan, 1992 (unpublished).
[2] S. A. Kazantsev and J.-C. Hénoux, *Polarization Spectroscopy of Ionized Gases* (Kluwer, Academic, Boston, 1995).
[3] D. W. O. Heddle and J. W. Gallagher, Rev. Mod. Phys. **61**, 221 (1989).
[4] D. W. O. Heddle, Contemp. Phys. **17**, 443 (1976).
[5] P. Hammond, W. Karras, A. G. McConkey, and J. W. McConkey, Phys. Rev. A **40**, 1804 (1989).
[6] C. Norén, J. W. McConkey, P. Hammond, and K. Bartschat, Phys Rev. A **53**, 1559 (1995).
[7] I. C. Percival and M. J. Seaton, Philos. Trans. R. Soc. London Ser. A **251**, 113 (1958).
[8] K. Blum, *Density Matrix Theory and Applications* (Plenum, New York, 1981).
[9] G. F. Hanne and J. Kessler, J. Phys. B **9**, 791 (1976).
[10] G. F. Hanne, K. Wemhoff, A. Wolcke, and J. Kessler, J. Phys. B **14**, L507 (1981).
[11] H. G. M. Heideman, W. van der Water, and L. J. M. Moergestel, J. Phys. B **13**, 2801 (1980).
[12] S. J. Buckman and C. W. Clark, Rev. Mod. Phys. **66**, 539 (1994).
[13] F. H. Read, J. N. H. Brunt, and G. C. King, J. Phys. B **9**, 2209 (1976).
[14] T. Noro, F. Sasaki, and H. Tatewaki, J. Phys. B **12**, 2217 (1979).
[15] P. C. Ohja, P. G. Burke, and K. T. Taylor, J. Phys. B **15**, L507 (1982).

[16] C. W. Clark and K. T. Taylor, J. Phys. B **15**, L213 (1982).
[17] A. Wolcke, K. Bartschat, K. Blum, H. Borgmann, G. F. Hanne, and J. Kessler, J. Phys. B **16**, 639 (1983).
[18] E. Baranger and E. Gerjuoy, Proc. Phys. Soc. London **72**, 326 (1958).
[19] M. Weissbluth, *Atoms and Molecules (Student Edition)* (Academic, Toronto, 1978), p. 31.
[20] C. W. Clark, in *Electron Correlation Effects and Negative Ions*, edited by T. Anderson (Aarhus University Press, Aarhus, Denmark, 1984), p. 49.
[21] K. Bartschat, K. Blum, G. F. Hanne, and J. Kessler, J. Phys. B **14**, 3761 (1981).
[22] W. Karras, M. Sc. thesis, University of Windsor, 1988 (unpublished).
[23] M. Uhrig, S. Hörnemann, M. Klose, K. Becker, and G. F. Hanne, Meas. Sci. Technol. **5**, 1239 (1994).
[24] J. N. H. Brunt, G. C. King, and F. H. Read, J. Phys. B **10**, 3781 (1977).
[25] S. J. Buckman, P. Hammond, G. C. King, and F. H. Read, J. Phys. B **16**, 4219 (1983).
[26] J. O. Phelps, M. H. Phillips, L. W. Anderson, and C. C. Lin, J. Phys. B **16**, 3825 (1983).
[27] C. Norén, Ph.D. thesis, University of Windsor, 1995 (unpublished).
[28] F. A. Sharpton, R. M. St. John, C. C. Lin, and F. E. Fajen, Phys. Rev. A **2**, 1305 (1970).
[29] N. C. Steph and D. E. Golden, Phys. Rev. A **26**, 148 (1982).
[30] M. H. Phillips, L. W. Anderson, and C. C. Lin, Phys. Rev. A **32**, 2117 (1985).
[31] J. C. McConnell and B. L. Moiseiwitsch, J. Phys. B **1**, 406 (1968).
[32] R. A. Bonham, J. Phys. B **15**, L361 (1982).